Annals of Biomedical Engineering, Vol. 26, pp. 260–267, 1998
Printed in the USA. All rights reserved.

0090-6964/98 $10.50 + .00

An Adaptive Filter to Reduce Cardiogenic Oscillations on Esophageal Pressure Signals

THOMAS F. SCHUESSLER, STEWART B. GOTTFRIED, PETER GOLDBERG, ROBERT E. KEARNEY, and JASON H. T. BATES

Meakins-Christie Laboratories, Montréal Chest Hospital Research Institute and Department of Biomedical Engineering, McGill University, Montréal, Québec, Canada

(Received 24 January 1997; accepted 9 July 1997)

Abstract—Measurements of pressure swings in the esophagus (P_{es}) can be used to estimate variables of clinical importance, e.g., intrinsic positive end-expiratory pressure ($PEEP_i$). Unfortunately, cardiogenic oscillations frequently corrupt P_{es} and complicate further analysis. Due to significant band overlap with the respiratory component of P_{es}, cardiogenic oscillations cannot be suppressed adequately using standard filtering techniques. In this article, we present an adaptive filter that employs the electrocardiogram to identify and suppress the cardiogenic oscillations. This filter was tested using simulated data, where the variance accounted for relative to the simulated respiratory pressure swings increased from as low as 55% for the unfiltered P_{es} signal to over 95% when the adaptive filter was used. In patient data, the adaptive filter reduced the apparent cardiogenic oscillations without noticeably distorting the sharp deflections in P_{es} due to respiration. Furthermore, the filter suppressed peaks in the Fourier transform of P_{es} at integer multiples of the heart rate, while the remaining frequencies remained largely unchanged. During stable breathing, the standard deviation of $PEEP_i$ was reduced by between 44% and 71% in these four patients when the filter was used. We conclude that our filter removes a significant fraction of the cardiogenic oscillations that corrupt records of P_{es}. © *1998 Biomedical Engineering Society.* [S0090-6964(98)00102-7]

Keywords—Pulmonary monitoring, Intrinsic PEEP, Work of breathing.

INTRODUCTION

Respiratory pressure swings in the esophagus (P_{es}) can be measured using an esophageal balloon, i.e., a small elastic balloon attached to the end of a small plastic catheter placed in the mid-thoracic section of the esophagus. Provided that the esophageal balloon is adequately placed and inflated, swings in P_{es} reflect swings in pleural pressure (P_{pl}) during spontaneous breathing.[1,2,5,6] Measurements of P_{es} can be used to separate estimates of respiratory mechanics into lung and chest wall compartments,[4,8] to evaluate variables of clinical importance such as dynamic intrinsic PEEP ($PEEP_{i,dyn}$) and inspiratory work of breathing (W_{insp}),[3,7,13,16] and to estimate the patient's muscular and/or neural drive.[11,12]

Since the esophageal balloon is placed in close proximity to the heart, P_{es} recordings often contain cardiogenic oscillations. These are components of P_{es} that are not directly related to respiration, but originate from pressure changes within the pericardium and the aorta that are communicated to the esophageal balloon. Cardiogenic oscillations can be large enough to significantly complicate processing of the P_{es} signal. For example, we have recently demonstrated in a computer simulation that cardiogenic oscillations on P_{es} may introduce substantial errors to estimates of $PEEP_{i,dyn}$ and W_{insp}.[14] Similarly, cardiogenic oscillations reduce the goodness of model fits when the mechanical properties of the lungs and chest wall are identified using P_{es}. Unfortunately, cardiogenic oscillations cannot be removed from P_{es} signals by simple low pass filtering because their frequency content overlaps that of the respiratory signal.

We have recently presented an adaptive filter that reduces the effects of cardiogenic oscillations on esophageal pressure.[15] In this article, we further develop this filter and validate its performance using both simulated data and records obtained from four patients in a respiratory intensive care unit (ICU). Finally, we demonstrate the effects of the adaptive filter on estimates of $PEEP_{i,dyn}$ in these patients.

METHODS

The Adaptive Filter

In order to develop the adaptive filter presented in this study, we model P_{es} as the sum of pressure swings due to respiration (P_{resp}) and the undesired cardiogenic oscillation pressure (P_{CGO}), as illustrated in Fig. 1(a). The

Address correspondence to Dr. Jason H. T. Bates, Meakins-Christie Laboratories, McGill University, 3626 Rue Street, Urbain, Montréal, Québec H2X 2P2, Canada. Electronic mail: jason@meakins.lan.mcgill.ca

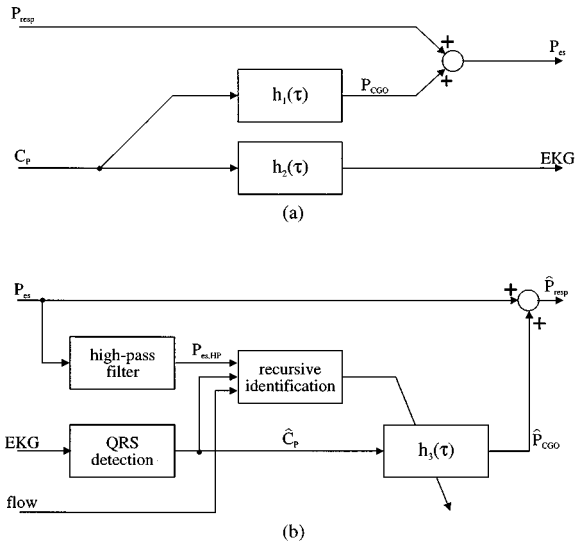

FIGURE 1. (a) Model of the origin of cardiogenic oscillations employed to develop the adaptive filter. (b) Structure of the adaptive filter.

linear dynamic system described by the impulse response function $h_1(\tau)$ relates P_{CGO} to the series of impulses generated by the cardiac pacemaker in the sinoatrial (SA) node (C_P). P_{CGO} contains very little power at frequencies below the heart rate (HR), while P_{resp} is likely to contain significant power below the HR because the respiratory rate (RR) is generally less than the HR. Therefore, P_{es} can be considered to be entirely determined by P_{resp} in the frequency band from 0 Hz to slightly below the HR, but to contain significant cardiogenic oscillations at and above the HR. A second impulse response, $h_2(\tau)$, translates C_P into voltage swings on the body surface that can be measured as an electrocardiogram (EKG).

In our adaptive filter, a number of quantities are smoothed by recursively calculating an exponentially weighted running mean according to

$$\overline{x_k} = \alpha \overline{x_{k-1}} + (1-\alpha)x_k, \tag{1}$$

where $\overline{x_k}$ is the estimate of the mean obtained up to sample k. α is often referred to as a forgetting factor, and must range between 0 and 1. If x is sampled uniformly, this estimator becomes equivalent to a single-pole low-pass filter, and α is related to the time constant of the finite memory, τ, by the equation

$$\tau = -\frac{\Delta t}{\ln(\alpha)}, \tag{2}$$

where Δt is the sampling interval. If α is adequately chosen, this recursive estimator will track slow changes in x but average out rapid fluctuations and measurement noise.

Our adaptive filter is an adaptive noise canceller[19] with the structure shown in Fig. 1(b). In order to compute an estimate of P_{CGO} ($\hat{P}_{\mathrm{CGO}}$), we first generated a sequence of impulses representing the cardiac R-waves from a lead II EKG by thresholding the negative deflections of the EKG. The threshold value for the R-wave detection was set to 1.7 times the rms value of the EKG signal, which was smoothed recursively as described above with a forgetting factor of 0.97. Provided that $h_2(\tau)$ is stationary, this sequence of impulses represents an estimate of C_P, i.e.,

$$\hat{C}_P \approx C_P(t-\tau_2), \tag{3}$$

where τ_2 is the delay between the initiation of a heart beat in the SA node and its manifestation in the EKG. The HR was computed from the inverse R–R intervals and smoothed recursively using a forgetting factor of 0.9.

Next, we high-pass filtered P_{es} using a two-sided 256th-order finite impulse response (FIR) filter with a constant group delay. The cutoff frequency (f_C) of this filter was adjusted to 0.6 times the identified HR. Thus, the high-pass filtered P_{es} signal ($P_{\mathrm{es,HP}}$) still contained the complete and undistorted P_{CGO}, but suppressed the low frequency components of P_{resp} that might complicate the following processing steps. The two sided high-pass filter introduced a delay of 128 data points from the moment that data were sampled to the point when filtered values were available. Since all data were sampled at 100 Hz, the time delay amounted to 1.28 s.

Assuming linearity, we have that

$$P_{\mathrm{CGO}} = h_1(\tau-\tau_2) * \hat{C}_P, \tag{4}$$

where * denotes convolution. In order to calculate $\hat{P}_{\mathrm{CGO}}$, we recursively estimated a third impulse response, $h_3(\tau)$, according to

$$h_3^{(k+1)}(\tau) = \alpha h_3^{(k)}(\tau) + (\alpha-1)P_{\mathrm{es,HP}}^{(k)}(t), \tag{5}$$

where α again is the forgetting factor, and $P_{\mathrm{es,HP}}^{(k)}$ is the segment of $P_{\mathrm{es,HP}}$ that falls into the kth R–R interval. Assuming that there is no phase-locking between the heart rate and the breathing cycle, and provided that α is sufficiently large, components of $h_3(\tau)$ that originate from P_{resp} are averaged out so that $h_3(\tau)$ effectively provides an estimate of $h_1(\tau-\tau_2)$. Using $h_3(\tau)$, we computed $\hat{P}_{\mathrm{CGO}}$ and subtracted it from P_{es} in order to obtain the final estimate of P_{resp}, i.e.,

$$\hat{P}_{\mathrm{resp}} = P_{\mathrm{es}} - \hat{P}_{\mathrm{CGO}} = P_{\mathrm{es}} - h_3(\tau) * \hat{C}_P. \tag{6}$$

The choice of the forgetting factor α in Eq. (5) is a crucial determinant of the algorithm's performance. If α is too small then $h_3(\tau)$ becomes sensitive to measurement noise, and contributions to $P_{\text{es,HP}}$ that originate from P_{resp} are not efficiently averaged out. On the other hand, large values of α limit the filter's ability to adapt to changes in $h_1(\tau)$ over time. Part of this problem can be overcome by using the adaptive scheme of Wellstead and Sanoff[18] to update α at each iteration. Briefly, this scheme recursively tracks the residuals with a finite memory. When the residuals are persistently large, a change in the underlying dynamics is assumed and α is decreased. Conversely, α is increased to reduce the sensitivity to measurement noise in the case of consistently small residuals. This scheme has been applied successfully to fit models of respiratory mechanics to pressure and flow data.[10]

While the scheme of Wellstead and Sanoff alters α appropriately in the case of changing underlying dynamics, it fails in the presence of increased band overlap, i.e., when the frequency content of P_{CGO} increasingly overlaps that of P_{resp}. Band overlap also increases the variability between P_{CGO} and $P_{\text{es,HP}}$, but requires an increase in rather than a reduction of α in order to properly average out the contributions of P_{resp} in Eq. (5). We are thus faced with conflicting possibilities when $\hat{P}_{\text{CGO}}$ and $P_{\text{es,HP}}$ do not match well: it may be that the underlying dynamics are varying in which case α should be decreased, or it may be due to band overlap in which case α should be increased. However, some *a priori* information to estimate the prominence of band overlap can be obtained from the relative values of the HR and the RR. We developed a modified scheme to adaptively update α at each interval k that encapsulates this *a priori* information. We start with an expression similar to the scheme by Wellstead and Sanoff, i.e.,

$$\alpha_k = 1 - \frac{\Delta_k}{1+\Delta_k}. \tag{7}$$

However, Δ in this case is a function of the residuals, the heart rate, and the respiratory rate that is recursively updated according to

$$\Delta_k = \gamma\Delta_{k-1} + (1-\gamma)\,\frac{\|P_{\text{es,HP}}^{(k)} - h_3^{(k)}\|}{\|h_3^{(k)}\|} \times \exp(\kappa_1^{-1}\text{HR/RR} + \kappa_3), \tag{8}$$

where γ is another forgetting factor, and $\|.\|$ denotes a quadratic norm. The exponential term in Eq. (8) was chosen empirically on the basis of preliminary computer simulations and effectively determines the range over which the scheme can modify α. When the HR is close to the RR, the exponential term in Eq. (8) is small. This in turn causes Δ_k to remain small, so that α_k in Eq. (7) is close to unity, biasing the algorithm towards long memory. The effects of band overlap can thus be averaged out. Conversely, as the HR becomes much greater than the RR, the exponential term in Eq. (8) increases. This allows Δ_k to be large and the memory to be short when $P_{\text{es,HP}}$ consistently differs significantly from h_3. The filter can then adapt rapidly to changes in P_{CGO}. The constants in Eq. (8) were set to $\gamma = 0.8$, $\kappa_1 = 0.5$, and $\kappa_2 = -5$. Small changes in these parameters hardly affected the overall outcome, indicating that this scheme is robust towards slight misadjustments of γ, κ_1, and κ_2. The RR was computed from the intervals between the onset of inspiratory flow and smoothed recursively with a forgetting factor of 0.6.

Computer Simulations

To test our adaptive filter, we simulated P_{es} signals contaminated with cardiogenic oscillations using a nonlinear, viscoelastic model of a spontaneously breathing patient. This model has previously been used to evaluate the effect of cardiogenic oscillations on PEEP_i.[14] In order to introduce a physiologically reasonable variability in P_{CGO} over time, we extended this model by making the magnitude of P_{CGO} depend on volume according to

$$P_{\text{CGO}} = k_1 \exp\left(k_2\,\frac{\text{FRC} - V(t)}{\text{FRC}}\right)\tilde{P}_{\text{CGO}}. \tag{9}$$

Here, FRC is the functional residual capacity, $V(t)$ is the absolute lung volume at any point in time, and $\tilde{P}_{\text{CGO}}$ is the preliminary, volume independent cardiogenic oscillation wave form. The constants k_1 and k_2 were chosen to be 10 cm H_2O and 5, respectively. This functional form of the volume dependence was chosen arbitrarily to reproduce physiologically reasonable magnitudes of P_{CGO}.

We simulated eight patients with the RRs and HRs shown in Table 1. These values were chosen to produce degrees of band overlap spanning the range likely to be observed in real patients. The inspiratory drive was adjusted to produce normal minute ventilations between 5.5 and 7.2 L/min, and expiratory muscle activity was absent in all eight simulated patients. All other model parameters were chosen equal to the population means listed in Table 1 of Ref. 14. Patients 1–4 had very rapid shallow breathing patterns with a RR of 40 breaths/min. The simulations were designed such that band overlap was most pronounced in patient 1, where the HR with 54.7 bpm was only 37% higher than the RR. In contrast, patients 5–8 breathed deeply with a RR of 10 breaths/min. In these patients, band overlap was less prominent, but the effects of the volume dependence of P_{CGO} became more important due to the larger tidal volume.

TABLE 1. Variance accounted for using the filtered and unfiltered P_{es} in eight simulated patients.

Simulated patient	1	2	3	4	5	6	7	8	
Heart rate	54.7	74.7	139.3	199.3	54.7	74.7	139.3	199.3	min^{-1}
Respiratory rate	40	40	40	40	10	10	10	10	min^{-1}
VAF[a] unfiltered	57.9	54.5	64.5	76.2	90.2	89.4	91.7	94.4	%
VAF filtered	95.4	97.7	97.8	97.9	98.5	98.7	98.9	99.4	%

[a]Variance accounted for.

Three min of data were simulated for each patient, and the first 2 min of data were discarded in order to ensure that the steady state of the simulation had been reached, and to allow the filter to adapt. From the last minute of data, we evaluated the VAF by both P_{es} and $\hat{P}_{resp}$ with respect to the true P_{resp} in order to quantify the reduction of the cardiogenic oscillation achieved by our adaptive filter.

Patient Data

We also applied our adaptive filter to recordings of P_{es}, flow and EKG that had been obtained from four patients receiving ventilatory support in the ICU of the Montreal Chest Hospital. Each data collection protocol was approved by the local ethics committee, and informed consent was obtained from all subjects. All signals were amplified and anti-aliasing filtered at 30 Hz using 6th order Bessel low-pass filters and digitized at a sampling rate of 100 Hz. The correct position of the esophageal balloon was verified prior to data collection by a standard occlusion test.[1] Table 2 summarizes the characteristics of each patient.

From each patient record, we chose a data segment for further analysis that (i) started a minimum of 60 s after the beginning of data collection to permit time for the filter to adapt, (ii) showed a relatively stable breathing pattern over a period of at least 10 breaths, and (iii) did not contain any esophageal spasms or EKG artifacts. For each analysis segment, we computed the magnitude of the 2048-point Fourier transform (FT) of both the unfiltered and the filtered P_{es} using a Hamming window with 50% overlap. Using the same segments, $PEEP_{i,dyn}$ was estimated automatically for each breath as the deflection in P_{es} from its end-expiratory plateau value ($P_{es,plateau}$) to the onset of inspiratory flow. $PEEP_{i,dyn}$ was corrected for the trigger threshold of the ventilator by subtracting the deflection in airway opening pressure that occurred simultaneously with the deflection in P_{es}. $P_{es,plateau}$ was detected as the point closest to the onset of inspiratory flow at which the five-point derivative of P_{es} was within 0.1% of its minimum value over the preceding expiration. The onset of inspiratory flow was identified by extrapolating backwards to zero flow from the points at which inspiratory flow amounted to 50 and 100 mL/s. This procedure was carried out using both the unfiltered and the filtered P_{es}, and the mean and standard deviation of $PEEP_{i,dyn}$ were computed in each case.

All simulations and data analysis were carried out using the MATLAB 4.2/SIMULINK 1.3 mathematical software package (The Mathworks, Nattick, MA).

RESULTS

Simulated Data

Figure 2 shows samples of the simulated P_{resp} and P_{es} and the resulting $\hat{P}_{resp}$ traces for simulated patients 1 (top) and 8 (bottom). In both patients, the unfiltered P_{es} (center panels) differs significantly from the simulated

TABLE 2. Patient characteristics.

Patient	Sex	Age	Diagnosis	Ventilator mode	Heart rate	Respiratory rate
A	male	6	COPD/Pneumonia	CPAP[b] 5 cm H_2O	126 min^{-1}	22 min^{-1}
B	female	57	COPD[a]	PAV[c]+PEEP[e] 3 cm H_2O	104 min^{-1}	15 min^{-1}
C	male	64	COPD[a]	PAV[d]+PEEP[e] 4 cm H_2O	87 min^{-1}	32 min^{-1}
D	female	69	COPD[a]	PSV[d] 12 cm H_2O + PEEP[e] 5 cm H_2O	106 min^{-1}	4.7 min^{-1}

[a]Chronic obstructive pulmonary disease.
[b]Constant positive airway pressure.
[c]Proportional assist ventilation.
[d]Pressure support ventilation.
[e](Applied) Positive end-expiratory pressure.

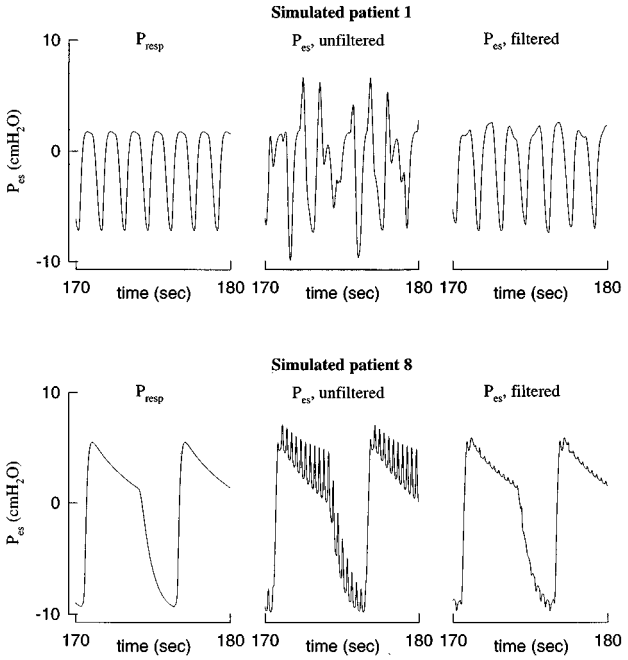

FIGURE 2. Simulated data for simulated patients 1 (top) and 8 (bottom). The filtered P_{es} traces (right panels) reproduce the simulated P_{resp} traces (left panels) with much greater accuracy than the unfiltered P_{es} traces (center panels).

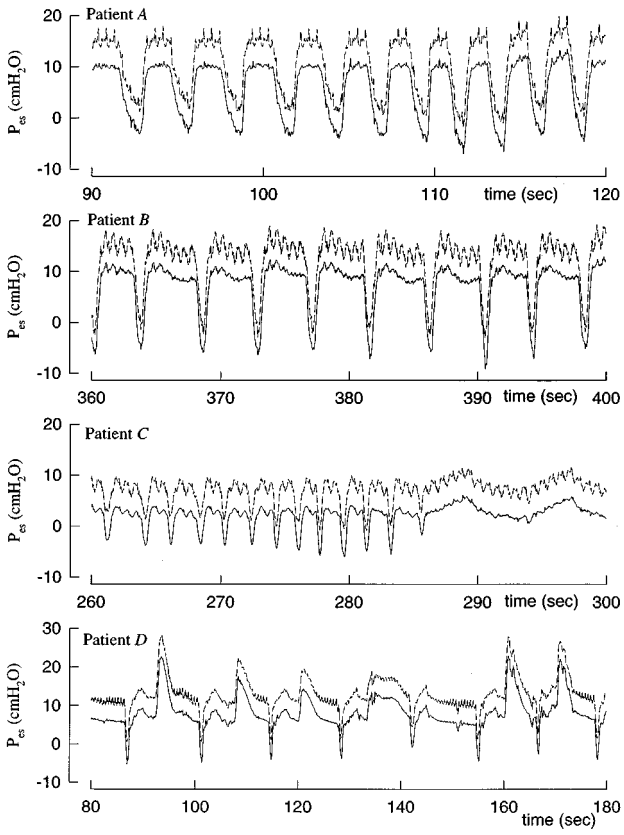

FIGURE 3. Sample traces from the four patients studied. Dashed lines: Unfiltered P_{es} signals. (Solid lines) Adaptively filtered P_{es} signal (shifted downward by 5 cm H_2O to separate the curves). (Patient A) COPD/pneumonia patient on continuous positive airway pressure (CPAP) of 5 cm H_2O. (Patient B) COPD patient on proportional assist ventilation (PAV). (Patient C) COPD patient on PAV with a very high respiratory rate of 32 breaths/min. At $t=290$ s, this patient was switched to pressure support ventilation (PSV), causing the respiratory rate to instantaneously drop to 8 breaths/min. (Patient D) COPD patient on PSV with a very low respiratory rate of 4.7 breaths/min. This patient showed an abnormal recruitment of the expiratory muscles.

P_{resp} (left panels). In patient 1 where band overlap was most pronounced, the effects of the cardiogenic oscillations were suppressed to a large extent, but not entirely in the filtered P_{es} signal (top right panel). In the filtered P_{es} trace of patient 8 where volume dependence was more pronounced (bottom right panel), most of the cardiogenic oscillations were suppressed.

The VAFs for both P_{es} and $\hat{P}_{resp}$ are shown in the bottom two rows of Table 1. When the RR was 10 breaths/min, P_{es} accounted for around 89% to 94% of the variance of P_{resp}. This number dropped as low as 55% when the RR was raised to 40 breaths/min and band overlap became more prominent. $\hat{P}_{resp}$ produced a substantially greater VAF in all eight cases, with a minimum of 98.5% at a RR of 10 and a minimum of 95.4% at a RR of 40.

Patient Data

Figure 3 shows samples of the unfiltered (dashed lines) and filtered (solid lines) P_{es} for each of the four ICU patients studied. In all four graphs, the filtered P_{es} trace was shifted downward by 5 cm H_2O to separate the graphs. Except for patient C, the data shown in Fig. 3 lie completely within the segments used to compute the power spectrum and to estimate $PEEP_i$. For patient C, the analysis segment ended at $t=290$ s, when the patient was switched from proportional assist ventilation to pressure support ventilation. At this point, the RR of patient C dropped from 32 breaths/min to 8.3 breaths/min. Figure 3 shows this transition to illustrate the performance of our adaptive filter over a change in ventilatory conditions. Patient D had a large tidal volume at a very low RR of 4.7 and showed abnormal positive deflections in P_{es}. Analysis of concurrently recorded airway pressure and flow traces suggested that these were bursts of expiratory muscle recruitment.

In Fig. 4, the magnitudes of the FT of the unfiltered (dashed lines) and filtered (solid lines) P_{es} signals of all four patients are plotted against the frequency normalized to the heart rate. Thus, on the abscissa of each plot, the heart rate occurs at a value of one and its harmonics occur at integer values greater than one. In all cases, the

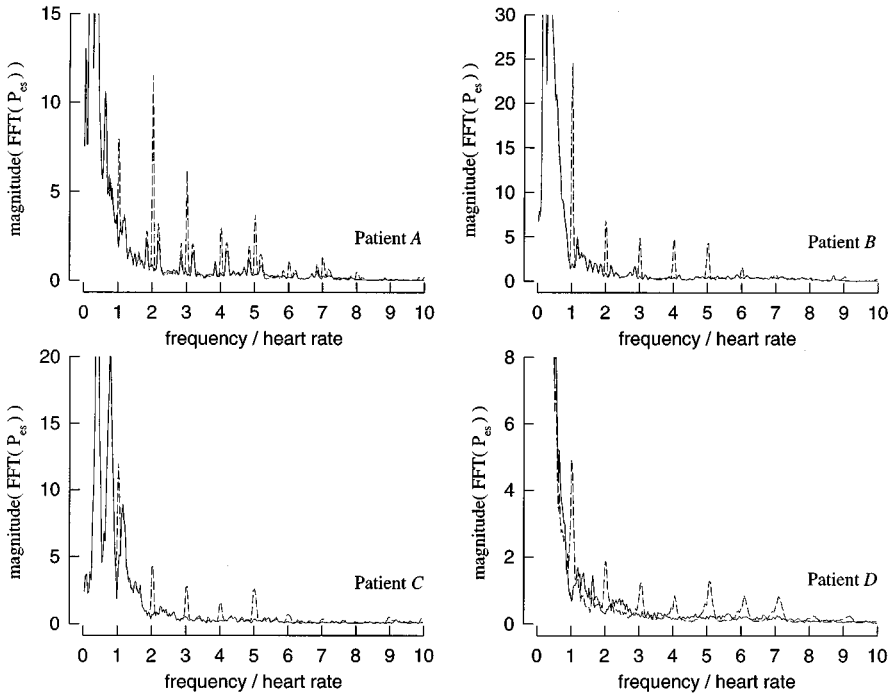

FIGURE 4. Magnitude of the Fourier transform of both the unfiltered (dashed lines) and filtered (solid lines) esophageal pressure traces for all four patients, plotted against the frequency normalized to the heart rate. The Fourier transform was computed using a moving 2048-point Hamming window with 50% overlap. The filter removed transients in the Fourier transform at the heart rate and its harmonics (at integer values on the abscissa).

FT of the unfiltered P_{es} signal showed spikes at the heart rate and its harmonics that did not occur in the FT of the filtered P_{es} signal.

The mean and standard deviation of $PEEP_{i,dyn}$ for each patient are shown in Table 3. The standard deviation of $PEEP_{i,dyn}$ was less for the filtered than for the unfiltered P_{es} signal in all patients. The mean $PEEP_{i,dyn}$ dropped in three patients and increased in one patient when the filtered P_{es} signal was used.

DISCUSSION

In the present study, we have described in detail an adaptive filter to suppress the cardiogenic oscillations that complicate the processing of P_{es} signals. We tested this filter in eight simulated patients with a wide range of heart and respiratory rates. In all eight cases, $\hat{P}_{resp}$ reproduced the P_{resp} with substantially greater accuracy than the unfiltered P_{es}. The VAF of $\hat{P}_{resp}$ with respect to P_{resp} was lowest in simulated patient 1 where band overlap was most pronounced, but exceeded 95% in all simulated patients.

We also tested the adaptive filter in four patients receiving mechanical ventilatory support in the ICU. The performance of the adaptive filter is more difficult to evaluate in patients because P_{resp} is unknown and cannot be used as a reference. However, our adaptive filter always reduced the apparent cardiogenic oscillations without noticeably distorting the sharp deflections due to respiration (Fig. 3). In the Fourier domain, the filter suppressed transients at integer multiples of the heart rate

TABLE 3. Intrinsic PEEP obtained from the unfiltered and the filtered esophageal pressure signal (mean±standard deviation).

Patient	Length of analyzed data segment	$PEEP_{i,dyn}$[a] (unfiltered P_{es})	$PEEP_{i,dyn}$[a] (filtered P_{es})
A	100 s (36 breaths)	0.54±1.06 cm H_2O	0.18±0.31 cm H_2O
B	100 s (25 breaths)	1.54±1.59 cm H_2O	1.11±0.57 cm H_2O
C	50 s (24 breaths)	2.06±1.11 cm H_2O	1.06±0.56 cm H_2O
D	120 s (10 breaths)	2.56±1.64 cm H_2O	3.76±0.92 cm H_2O

[a]Dynamic intrinsic positive end-expiratory pressure.

that presumably represent the harmonics of P_{CGO}. Otherwise, the FT of the filtered P_{es} signal closely resembled the FT of the unfiltered P_{es} signal. These results indicate that our adaptive filter adequately reduces the cardiogenic oscillations in P_{es} without unduly distorting the respiratory pressure swings.

Finally, we applied our adaptive filter to the computerized estimation of $PEEP_{i,dyn}$ using our previously described algorithm.[14] The mean $PEEP_{i,dyn}$ was reduced in three patients and increased in one patient. However, the standard deviation of $PEEP_{i,dyn}$ was reduced by 44% to 71% (mean 57%) in all four patients when the filtered P_{es} was used. This suggests, as one would expect, that part of the variability of the $PEEP_{i,dyn}$ obtained from the unfiltered P_{es} was not due to variability in the patient's breathing pattern, but rather to the cardiogenic oscillations. As it is improbable that the patients were perfectly stable over the analysis period, it seems likely that part of the remaining variability must have been physiologic.

To develop our adaptive filter, we assumed P_{es} to represent the sum of two independent and uncorrelated pressure signals, namely P_{resp} and P_{CGO}. Clearly, this is not a precise account of events. First, the coupling between the heart and the esophageal balloon is likely to be volume dependent. This would cause P_{CGO} to be entrained with respiration in patients with large tidal volumes. However, we found our filter to perform well in our computer simulations even when the simulated P_{CGO} was markedly volume dependent (simulated patients 5–8). The filter also performed well in patient D where the amplitude of the cardiogenic oscillations appeared to increase during expiration as lung volume decreased.

Second, since the beating heart is located within the thoracic cavity, cardiac pressure swings are not only communicated directly to the esophageal balloon, but also contribute to the pleural pressure swings. Depending on the application, this indirect contribution of the heart to P_{es} may be considered part of the respiratory pressure swings because it contributes to the transpulmonary pressure and hence influences flow. Alternatively, it may be considered artifactual because it does not originate from the respiratory musculature. In any case, this indirect contribution of the heart is likely to contribute much less to the cardiogenic oscillations on P_{es} than the direct coupling from the heart to the esophageal balloon.

The identification of the transfer function $h_3(\tau)$ would, in general, require the utilization of time-domain system identification techniques[9,17] between P_{es} and $\hat{C}_P$. However, the input signal to h_3 is reduced to a single impulse function when each $R-R$ interval is processed independently. Provided that the delay between a cardiac event and its manifestation in P_{es} is much shorter than the duration of an $R-R$ interval, the segment of P_{es} that corresponds to the $R-R$ interval constitutes the impulse response, obliterating the need for computationally expensive deconvolution.

In summary, we have described an adaptive filter that reduces the cardiogenic oscillations on esophageal pressure traces. We have validated its performance in a computer simulation, and we have shown its effect in both the time and the frequency domain on data obtained from four ICU patients. Furthermore, we found the standard deviation of breath-by-breath estimates of $PEEP_{i,dyn}$, obtained from periods with seemingly stable breathing patterns, to be substantially reduced when the adaptive filter was used.

ACKNOWLEDGMENTS

This work was supported by the Medical Research Council of Canada, the Respiratory Health Network of Centres of Excellence, the J. T. Costello Memorial Research Fund, and the Montréal Chest Research Institute. J.H.T.B. is a Chercheur-Boursier of the Fonds de la Recherche en Santé du Québec.

REFERENCES

[1] Baydur, A., P. K. Behrakis, W. A. Zin, M. Jaeger, and J. Milic-Emili. A simple method for assessing the validity of the esophageal balloon technique. *Am. Rev. Respir. Dis.* 126:788–791, 1982.

[2] Chartrand, D. A., T. E. Ye, J. M. Maarek, and H. K. Chang. Measurement of pleural pressure at low and high frequencies in normal rabbits. *J. Appl. Physiol.* 63:1142–1146, 1987.

[3] Coussa, M. L., C. Guerin, N. T. Eissa, C. Corbeil, M. Chasse, J. Braidy, N. Matar, and J. Milic-Emili. Partitioning of work of breathing in mechanically ventilated COPD patients. *J. Appl. Physiol.* 75:1711–1719, 1993.

[4] Dechman, G. S., A.-M. Lauzon, and J. H. T. Bates. Mechanical behaviour of the canine respiratory system at very low lung volumes. *Respir. Physiol.* 95:119–129, 1993.

[5] Dechman, G. S., J. Sato, and J. H. T. Bates. Factors affecting the accuracy of esophageal balloon measurement of pleural pressure in dogs. *J. Appl. Physiol.* 72:383–388, 1992.

[6] Gillespie, D. J., Y.-L. Lai, and R. E. Hyatt. Comparison of esophageal and pleural pressure in the anesthetized dog. *J. Appl. Physiol.* 35:709–713, 1973.

[7] Gottfried, S. B., A. Rossi, and J. Milic-Emili. Dynamic hyperinflation, intrinsic PEEP, and the mechanically ventilated patient. *Intensive Crit. Care Dig.* 5:30–33, 1986.

[8] Guerin, C., M. L. Coussa, N. T. Eissa, C. Corbeil, M. Chasse, J. Braidy, N. Matar, and J. Milic-Emili. Lung and chest wall mechanics in mechanically ventilated COPD patients. *J. Appl. Physiol.* 74:1570–1580, 1993.

[9] Hunter, I. W., and R. E. Kearney. Two-sided linear filter identification. *Med. Biol. Eng. Comp.* 21:203–209, 1983.

[10] Lauzon, A.-M., and J. H. T. Bates. Estimation of time-varying respiratory mechanical parameters by recursive least squares. *J. Appl. Physiol.* 71:1159–1165, 1991.

[11] Marazzini, L., R. Cavestri, D. Gori, L. Gatti, and E. Longhini. Difference between mouth and esophagus occlusion pressure during CO_2 rebreathing in chronic obstructive pulmonary disease. *Am. Rev. Respir. Dis.* 118:1027–1033, 1978.

[12] Murciano, D., M. Aubier, S. Bussi, J. P. Derenne, R. Pariente, and J. Milic-Emili. Comparison of esophageal, tracheal and mouth occlusion pressure in patients with chronic obstructive pulmonary disease during acute respiratory failure. *Am. Rev. Respir. Dis.* 126:837–841, 1982.

[13] Petrof, B. J., M. Legare, P. Goldberg, J. Milic-Emili, and S. B. Gottfried. Continuous positive airway pressure reduces work of breathing and dyspnea during weaning from mechanical ventilation in severe chronic obstructive pulmonary disease. *Am. Rev. Respir. Dis.* 141:281–289, 1990.

[14] Schuessler, T. F., S. B. Gottfried, and J. H. T. Bates. A model of the spontaneously breathing patient: Applications to intrinsic PEEP and work of breathing. *J. Appl. Physiol.* 82:1694–1703, 1997.

[15] Schuessler, T. F., C. A. Volta, P. Goldberg, S. B. Gottfried, R. E. Kearney, and J. H. T. Bates. An adaptive filter for the reduction of cardiogenic oscillations on esophageal pressure signals. In: Annual International Conference IEEE Engineering Medical Biological Society, Montreal, Canada, 1995, Vol. 17, p. C-29.

[16] Smith, T. C., and J. J. Marini. Impact of PEEP on lung mechanics and work of breathing in severe airflow obstruction. *J. Appl. Physiol.* 65:1488–1499, 1988.

[17] Weiss, P. L., I. W. Hunter, and R. E. Kearney. Reduction of physiological signal contamination using linear filter identification. *Med. Biol. Eng. Comp.* 21:521–524, 1983.

[18] Wellstead, P. E., and S. P. Sanoff. Extended self-tuning algorithm. *Int. J. Control* 34:433–455, 1981.

[19] Widrow, B., and S. D. Stearns. Adaptive Signal Processing. Englewood Cliffs, NJ: Prentice-Hall, 1985.